

## Corrosion Inhibition in Chloride Solutions of Iron by 3-Amino-1,2,4-triazole-5-thiol and 1,1'-Thiocarbonyldiimidazole

El-Sayed M. Sherif<sup>1,2,\*</sup>

<sup>1</sup> Center of Excellence for Research in Engineering Materials (CEREM), College of Engineering, King Saud University, P. O. Box 800, Al-Riyadh 11421, Saudi Arabia

<sup>2</sup> Electrochemistry and Corrosion Laboratory, Department of Physical Chemistry, National Research Centre (NRC), Dokki, 12622 Cairo, Egypt

E-mail: [esherif@ksu.edu.sa](mailto:esherif@ksu.edu.sa)

Received: 24 April 2012 / Accepted: 15 May 2012 / Published: 1 June 2012

---

The inhibition of iron (Fe, 99.98%) corrosion after its immersion for 60 minutes in freely aerated 3.5% sodium chloride (NaCl) solutions by low concentrations of 3-amino-1,2,4-triazole-5-thiol (ATAT) and 1,1'-thiocarbonyldiimidazole (TCDI) was reported. The experimental tests in this work were open circuit potential (OCP), potentiodynamic polarization (PDP), chronoamperometric current-time (CT), electrochemical impedance spectroscopy (EIS), and in-situ Raman spectroscopy. The OCP and PDP curves indicated that the increased concentrations of ATAT or TCDI reduce the corrosion of Fe by shifting its corrosion potential towards the less negative values. CT tests for Fe at constant potential of  $-0.50$  V vs. Ag/AgCl for 120 min revealed that the ATAT and TCDI molecules inhibit the uniform and pitting corrosion. EIS Nyquist plots confirmed also that the presence of ATAT and TCDI and the increase of their concentrations decrease the corrosion of Fe through increasing the solution and charge transfer resistances. In-situ Raman spectra for iron in chloride solution containing ATAT and TCDI confirmed that the inhibition of iron corrosion is achieved by the adsorption of ATAT and TCDI molecules onto its surface.

---

**Keywords:** chloride solutions; corrosion inhibition; EIS; heterocyclic compounds; iron corrosion; Raman Spectroscopy

### 1. INTRODUCTION

Iron (Fe) plays a central role as one of the most widely used materials in our daily life because of its so many applications. The occurrence of iron corrosion in corrosive environments, especially those containing chloride, limits its uses. Thus, the corrosion and corrosion control of iron in harsh

media have reported by several researchers [1-6]. The protection of iron against corrosion in severe environments can be achieved by various ways. One of these is the use of corrosion inhibitors, which are usually chemical substances, when added in a small concentration to a corrosive medium, reduce effectively the corrosion of the metal and/or alloy [7-12].

Heterocyclic compounds such as azole derivatives have been reported to be effective inhibitors, especially those containing nitrogen, sulfur or oxygen atoms and aromatic rings or multiple bonds in their molecular structure are well known to inhibit the corrosion of metals in corrosive media [13-22]. The effectiveness of these compounds as corrosion inhibitors mainly depends on its functional groups, steric effects, electronic density of donor atoms, and p-orbital character of donating electrons [23-26]. The inhibition mechanism usually invokes their interactions with the metallic surfaces via their adsorption sites where polar functional groups are usually regarded as the reaction centers [27,28]. Here, the inhibitor molecules get bonded to the metal surface by chemisorption, physisorption, or complexation with the polar groups acting as the reactive centers in the molecules [29].

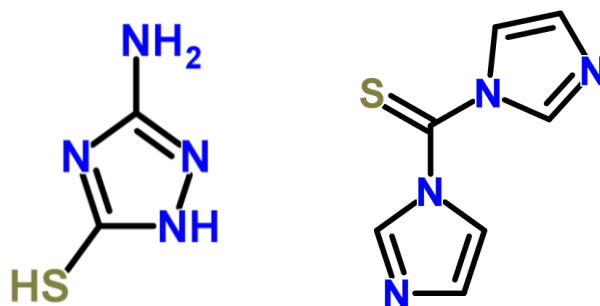


**Figure 1.** Chemical formula of ATAT (left) and TCDI (right), respectively.

The objective of the present work is study the corrosion of iron in freely aerated stagnant 3.5% sodium chloride solutions. The objective is also extended to compare the effects of 3-amino-1,2,4-triazole-5-thiol (ATAT) and 1,1'-thiocarbonyldiimidazole (TCDI) on the inhibition of iron corrosion in the aforementioned electrolyte. The chemical structure of ATAT and TCDI is shown in Fig. 1 from left to right, respectively. It is clearly seen from Fig. 1 that these compounds contain many donor nitrogen groups in addition to the presence of mercapto and amino groups in their heterocyclic structures. The presence of such these donor groups has been reported to facilitate and increase the adsorption probability of these compounds, which in turn protects the metal's surfaces through reducing the severity of the surrounding environments.

## 2. EXPERIMENTAL DETAILS

Sodium chloride (NaCl, Merck, 99%), 3-amino-1,2,4-triazole-5-thiol (ATAT, Sigma-Aldrich, 95%), 1,1'-thiocarbonyldiimidazole (TCDI, Alfa-Aesar, 94%), and absolute ethanol (C<sub>2</sub>H<sub>5</sub>OH, Merck, 99.9%) were used as received. An electrochemical cell with a three-electrode configuration was used

for electrochemical measurements; a single crystal iron rod (Fe, 99.98%, 9.5 mm in diameter), a platinum foil, and a Metrohm Ag/AgCl electrode (in 3 M KCl) were used as a working, counter, and reference electrodes, respectively. The iron electrode for electrochemical measurements was grinded successively with metallographic emery paper of increasing fineness of up to 800 grits, and then further with 5, 1, 0.5 and 0.3  $\mu\text{m}$  alumina slurries (Buehler). The electrode was thereafter cleaned with distilled water, degreased with acetone, and washed using distilled water again before finally dried with tissue paper.

Electrochemical experiments were performed by using a PARC Parstat-2273 Advanced Electrochemical System after immersing the iron electrode for 60 minutes in freely aerated stagnant 3.5% NaCl solution without and with  $1 \times 10^{-3}$ , and  $2 \times 10^{-3}$  M of ATAT and TCDI present. The potentiodynamic polarization curves were obtained by scanning the potential of iron from -1.20 V to 0.15 V vs. Ag/AgCl at a scan rate of 1 mV/s. Chronoamperometric current-time measurements were carried out by stepping a constant potential value of -0.50 V for 120 min.

The in-situ Raman spectroscopy investigations for iron in NaCl solutions alone and containing either  $1 \times 10^{-3}$  M ATAT or  $1 \times 10^{-3}$  M TCDI were collected using a special made Teflon cell. The iron electrode was polished and cleaned as for cases of iron rods used in the electrochemical measurements. The surface of this iron electrode was positioned 3 mm below the quartz window of the cell. The Ag/AgCl reference electrode was connected by a Lugging probe of 0.5 mm inner diameter and positioned 2 mm from the iron surface. The counter electrode was a 10 mm diameter Pt ring disc. The Jobin-Yvon T64000 Raman spectrometer was used in single spectrograph mode with a holographic dispersive grating of 600 g/mm, giving a resolution of  $2 \text{ cm}^{-1}$ . The iron surface in the electrochemical cell was analysed in back-scattering mode on the microscope stage of the Olympus confocal microscope attached to the spectrometer, with a long working distance 20x objective.

The potential-time curves were recorded from the first moment of iron immersion in all test solutions for 3600 seconds. For electrochemical impedance spectroscopy (EIS) experiments, the frequency was scanned at the open-circuit potential from 100 kHz to 0.1 Hz with an ac wave of  $\pm 5$  mV peak-to-peak overlaid on a dc bias potential, and the Nyquist plots were acquired using Powersine software at a rate of 10 points per decade change in frequency. All solutions were prepared using 99.0% doubly distilled water and only 1.0% ethanol (Vol. / Vol.) and all measurements were carried out at room temperature.

### 3. RESULTS AND DISCUSSION

#### 3.1. Potentiodynamic polarization (PDP) measurements

The PDP experiments were carried out to report the corrosion parameters including the cathodic ( $\beta_c$ ) and anodic ( $\beta_a$ ) Tafel slope, corrosion potential ( $E_{\text{Corr}}$ ), corrosion current density ( $j_{\text{Corr}}$ ), polarization resistance ( $R_p$ ), corrosion rate ( $K_{\text{Corr}}$ ) for iron electrode in 3.5% NaCl solution in absence and presence of ATAT and TCDI molecules. The PDP curves for iron electrode after its immersion for 60 min in 3.5% NaCl solutions without (1) and with (2)  $1 \times 10^{-3}$  M, and (3)  $2 \times 10^{-3}$  M (a) ATAT and (b)

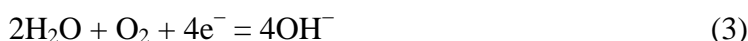
TCDI present, respectively are shown in Fig. 2. It is clearly seen from Fig. 2 that the currents recorded higher values for iron in the chloride solution alone, curves 1. It has been reported [2] that the anodic reaction for iron in sodium chloride solution is the dissolution of iron initially from Fe(0) into Fe(II),



The formed ferrous cations,  $\text{Fe}^{2+}$  is further oxidized under the application of high active potential values to ferric cations,  $\text{Fe}^{3+}$  according to the following reaction,



On the other hand, the cathodic reaction for metals in aerated near neutral solutions has been reported to be the oxygen reduction as follows [30-37],



This reaction consumes the electrons that are released during the dissolution of iron as shown in Eq. (1). Furthermore, the hydroxide ions resulting from reaction (3) react with the produced  $\text{Fe}^{2+}$  to form a deposit of  $\text{Fe}(\text{OH})_2$  as follows,

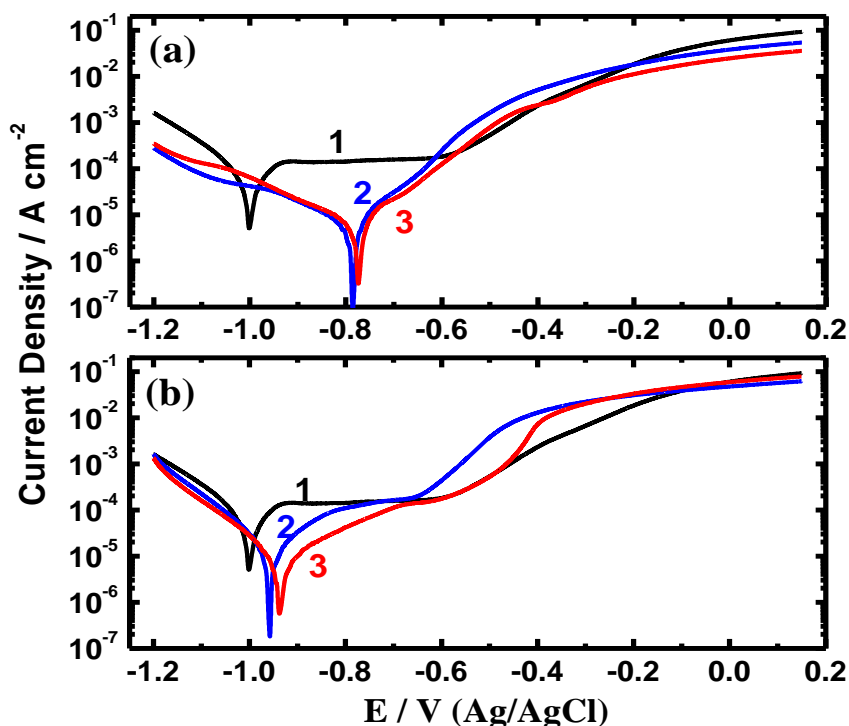
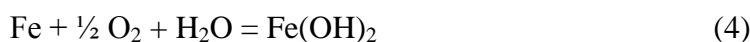


**Figure 2.** Potentiodynamic polarization curves for iron electrode after its immersion for 60 min in 3.5% NaCl solutions without (1) and with (2)  $1 \times 10^{-3}$  M, and (3)  $2 \times 10^{-3}$  M (a) ATAT and (b) TCDI present, respectively.

The formed ferrous hydroxide,  $\text{Fe}(\text{OH})_2$ , further transforms to magnetite ( $\text{Fe}_3\text{O}_4$ ) in the naturally aerated or oxygenated chloride solutions as can be seen by the reaction,



The formation of magnetite on the iron surface protects it from being attacked by the solution's chloride ions and could lead to the long passive region seen on curves 1 of Fig. 2. At more active potential values, the anodic branch shows a rapid increase in the output current, which explains the occurrence of pitting corrosion due to the breakdown of the formed magnetite passive layer. According to Darwish et al. [38], the dissolution of iron in concentrated NaCl solutions into ferrous cations occurs on multi-steps as follows,



**Table 1.** Corrosion parameters obtained from potentiodynamic polarization curves shown in Fig. 2 for iron in 3.5% NaCl solutions in absence and presence of ATAT and TCDI.

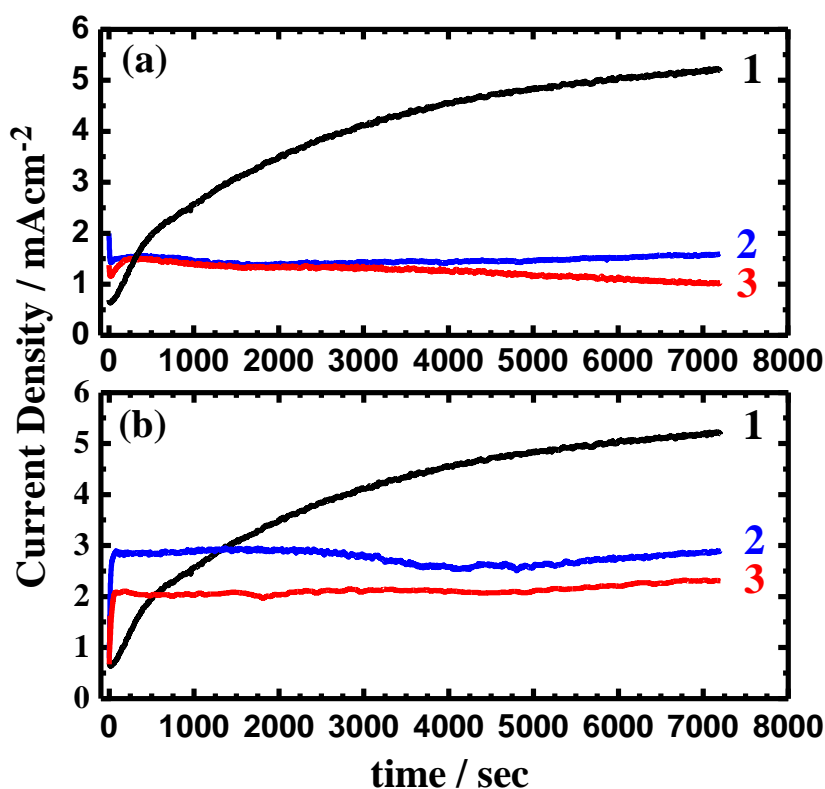
Solution	Parameter						
	$\beta_c/$ $\text{mVdec}^{-1}$	$E_{\text{Corr}}/$ $\text{mV}$	$j_{\text{Corr}}/$ $\mu\text{Acm}^{-2}$	$\beta_a/$ $\text{mVdec}^{-1}$	$R_p/$ $\text{k}\Omega\text{cm}^2$	$R_{\text{Corr}}/$ $\text{mmy}^{-1}$	IE/%
NaCl alone	120	-995	15	105	1.62	0.175	–
+ 1.0 mM ATAT	145	-790	4.9	120	5.83	0.057	67.4
+ 2.0 mM ATAT	160	-780	3.2	120	9.32	0.041	78.7
+ 1.0 mM TCDI	125	-955	5.2	125	5.22	0.062	65.3
+ 2.0 mM TCDI	130	-935	2.8	135	10.28	0.033	81.3

The presence of ATAT, Fig. 2a and TCDI, Fig. 2b, and the increase of their concentrations remarkably shifted the values of  $E_{\text{Corr}}$  to the less negative directions and decreased the values of  $j_{\text{Corr}}$ ,  $K_{\text{Corr}}$ , while increased the values of  $R_p$  for iron. This effect is due to the fact that ATAT and TCDI molecules decrease the severity of NaCl solutions and increase the corrosion resistance of iron surface. The values of  $\beta_c$ ,  $\beta_a$ ,  $j_{\text{Corr}}$ ,  $E_{\text{Corr}}$ ,  $R_p$ ,  $K_{\text{Corr}}$ , and the percentage of inhibition efficiency (IE%) obtained from Fig. 2 are listed in Table 1. The values of these parameters were calculated as has been reported in our previous studies [39-44]. As can be seen from Fig. 2 that the passive region recorded for iron in NaCl solutions alone, curves 1, decreased in the presence of ATAT and also in the presence of TCDI molecules and further with the increase of their concentrations. This can be attributed to the adsorption of ATAT and TCDI molecules on the iron surface, which leads to the prevention of iron dissolution and thus the prevention of iron oxides and chlorides to be formed on iron. This was also confirmed by

the increased values of IE% obtained on the iron surface for ATAT and TCDI with the increase of their concentrations.

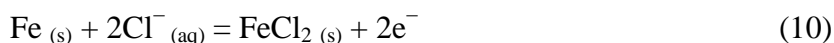
### 3.2. Chronoamperometric current-time (CT) measurements

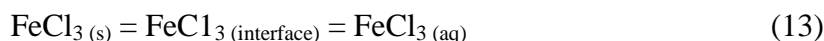
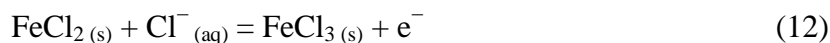
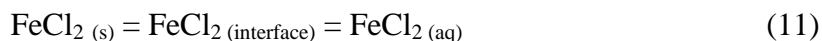
In order to shed more light on the dissolution of iron in 3.5% NaCl solutions and the effect of ATAT and TCDI molecules on the iron's uniform and pitting corrosion, CT experiments were carried out after 60 min immersion in the test solutions before applying an active potential value of -0.5 V vs. Ag/AgCl for 120 min. Fig. 3 shows the obtained CT curves for iron electrode that was immersed in the 3.5% NaCl solutions in (1) the absence and presence of (2)  $1 \times 10^{-3}$  and (3)  $2 \times 10^{-3}$  M of (a) ATAT and (b) TCDI, respectively.



**Figure 3.** Chronoamperometric curves obtained at -0.50 V vs. Ag/AgCl for iron electrode after its immersion for 60 min in 3.5% NaCl solutions without (1) and with (2)  $1 \times 10^{-3}$  M, and (3)  $2 \times 10^{-3}$  M (a) ATAT and (b) TCDI present, respectively.

The highest current values were recorded for Fe in chloride solution alone, Fig. 3 (curves 1); these values significantly increased with time, which is due to the continuous dissolution of iron by the severe attack of chloride ions and the active potential. The dissolution of iron at this condition has been reported [2,45,46] to occur according to the following reactions,





These reactions tell that the film formed on the iron surface is a mixed porous film of a precipitated ferrous chloride,  $\text{FeCl}_2$  and ferric chloride,  $\text{FeCl}_3$  compounds. Under the concentration gradients and the active applied potential, the  $\text{FeCl}_2$  and  $\text{FeCl}_3$  species at the interface diffuse through the porous film and the diffusion boundary layer and are then carried away to the bulk solution by convection. This in turn leads to the continuous uniform and pitting corrosion of iron with increasing the time of the applied potential on its surface.

The addition of  $1 \times 10^{-3}$  M ATAT as seen on curve 2 of Fig. 3a greatly decreased the absolute currents of iron and further decreasing of currents were recorded when the concentration of ATAT was increased to  $2 \times 10^{-3}$  M, Fig. 3a, curve 3. Moreover, the presence of ATAT stopped the increase of current with time. This can be explained on the bases that the ATAT molecules at these concentrations strongly inhibit and block the corrosion sites on the iron surface, which decreases the uniform corrosion and prevent the formation of pits. The addition of TCDI to the chloride solution, Fig. 3b, shows almost the same effect that was obtained by ATAT.

### 3.3. Open-circuit potential measurements and in-situ Raman Spectroscopy investigations

In order to show the potential behavior of iron in the different solutions and to see if the ATAT and TCDI molecules are spontaneously adsorbed on the iron surface, the OCP measurements were carried out. The OCP curves of the iron electrode in 3.5% NaCl solutions without (1) and with (2)  $1 \times 10^{-3}$  M, and (3)  $2 \times 10^{-3}$  M (a) ATAT and (b) TCDI present, respectively are depicted in Fig. 4. It is seen from Fig. 4, curves 1 that the potential of iron in chloride solution alone rapidly increased in the more negative direction in the first 300 sec, which is due to the dissolution of an oxide film was formed on iron in air before its immersion in the solutions. This dissolution occurs as a result of the chloride ions attack on the electrode surface. Increasing the time of the experiment showed a slight potential shift to the more negative values due to the continued chloride ions attack on iron surface.

The presence of  $1 \times 10^{-3}$  M ATAT, Fig. 4a (curve 2) shifted the initial potential of iron to a less negative value, after which it increased in the more negative direction. Increasing the ATAT concentration to  $2 \times 10^{-3}$ , Fig. 4a (curve 3) showed less negative potential shifts, especially with increasing the immersion time of iron. The addition of ATAT molecules thus shifts the OCP towards the less negative direction and this effect increases with increasing its concentration. It is seen from Fig. 4b also that the presence of TCDI and the increase of its concentration show almost similar OCP behavior to that obtained with ATAT at the same concentration. This agrees with the potential shifting trend obtained from polarization curves shown in Fig. 2 and listed in Table 1 and confirms that the presence of ATAT or TCDI and the increase of their concentrations inhibit the corrosion of iron in 3.5% NaCl solution.

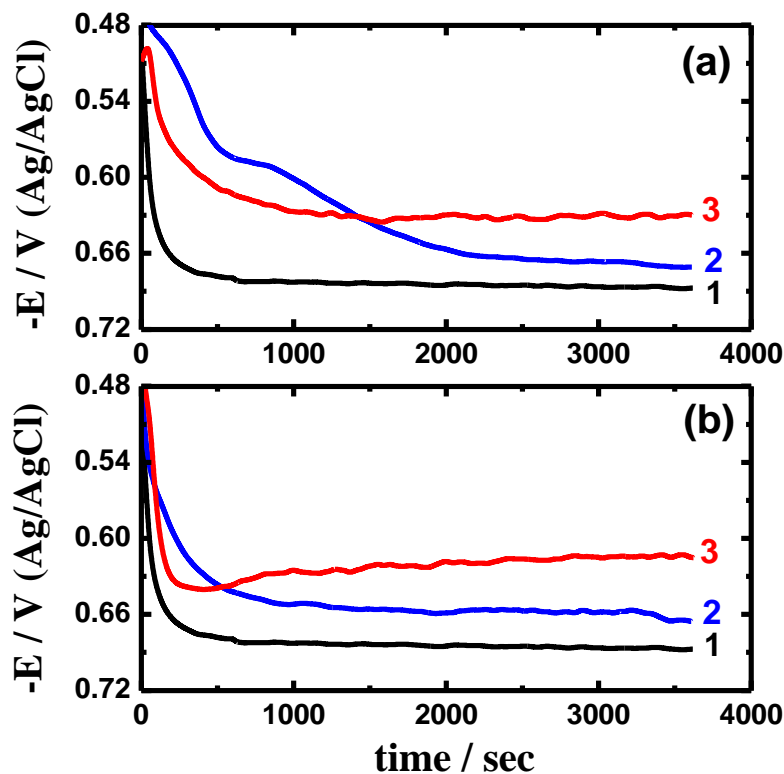


**Figure 4.** The variation of potential with time for iron electrode in 3.5% NaCl solutions without (1) and with (2)  $1 \times 10^{-3}$  M, and (3)  $2 \times 10^{-3}$  M (a) ATAT and (b) TCDI present, respectively.

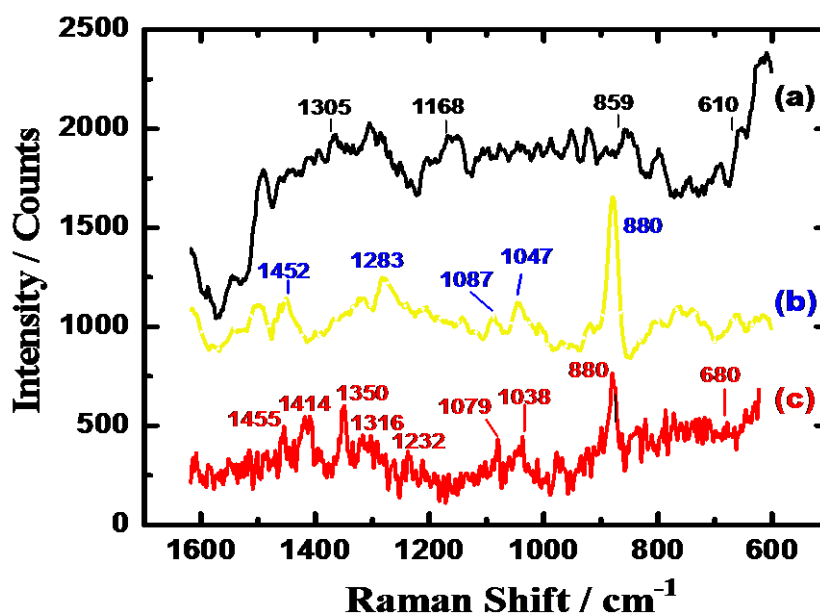


**Figure 5.** In-situ Raman spectra obtained on the iron surface after its immersion for 60 min in aerated 3.5% NaCl solutions without (a) and with (b)  $1 \times 10^{-3}$  M ATAT and (c)  $1 \times 10^{-3}$  M TCDI present, respectively.

In order to report the film formed on iron and to confirm whether the ATAT and TCDI molecules are indeed adsorbed as well as the molecular structure of the film formed on iron surface in

chloride solution alone and containing inhibitors, in situ Raman spectroscopy investigations were carried out. The in situ Raman spectra obtained on the iron surface after its immersion for 60 min in aerated 3.5% NaCl solutions without (a) and with (b)  $1 \times 10^{-3}$  M ATAT and (c)  $1 \times 10^{-3}$  M TCDI present, respectively are shown in Fig. 5. Fig. 5, curve a, shows only few weak bands appeared for iron in chloride solutions. For iron in chloride solution containing ATAT, Fig. 5 curve b, several bands were recorded at 880, 1047, 1087, 1283 and  $1452 \text{ cm}^{-1}$ . Moreover, the bands for iron in the chloride solution containing TCDI, Fig. 5, curve c, were appearing at 680, 880, 1038, 1079, 1232, 1316, 1350, 1414, and  $1455 \text{ cm}^{-1}$ .

The appearance of the weak band  $680 \text{ cm}^{-1}$  is related to a very thin iron oxide film, most probably magnetite ( $\text{Fe}_3\text{O}_4$ ) [47]. The appearance of the strong band at  $880 \text{ cm}^{-1}$  is due to ring breathing of both ATAT and TCDI. In addition to,  $1038$  and  $1046 \text{ cm}^{-1}$  in-plane ring-stretching vibrations of TCDI<sup>-</sup> and ATAT<sup>-</sup> anions interacting with Fe(II), respectively [17]. The  $-\text{N}=\text{N}-$  stretches at  $1078$  and  $1079 \text{ cm}^{-1}$  for ATAT and TCDI, respectively. For ATAT, the CH in plane bending at  $1276 \text{ cm}^{-1}$ ; and the triazole ring stretching at  $1448 \text{ cm}^{-1}$  [47]. For TCDI, the band  $1232 \text{ cm}^{-1}$  is due to C=C vibrations of the imidazole rings,  $1316$  and  $1414 \text{ cm}^{-1}$  are due to the interaction of the organic compound through away or another with the iron surface;  $1350 \text{ cm}^{-1}$  ring stretching due to N-H deformation [47–51]. The majority of the Raman mode assignments thus prove the presence of ATAT and TCDI or their complexes with iron in the formed film through their adsorption then polymerization onto the surface. This explains the positive potential shift for iron in chloride solutions containing ATAT and TCDI molecules as we have seen on Fig. 4.

### 3.5. Electrochemical impedance spectroscopy (EIS) measurements

In order to confirm the data obtained by dynamic polarization and chronoamperometry and to also determine kinetic parameters for electron transfer reactions at the iron/electrolyte interface, we carried out EIS experiments. The method was successfully employed to explain the corrosion and passivation phenomena of metals and alloys in different corrosive media [52–58]. Typical Nyquist plots for iron electrode after its immersion for 60 min in 3.5% NaCl solutions without (1) and with (2)  $1 \times 10^{-3}$  M, and (3)  $2 \times 10^{-3}$  M of (a) ATAT and (b) TCDI present, respectively are shown in Fig. 6. These spectra were analysed by fitting to the equivalent circuit model shown in Fig. 7. The parameters obtained by fitting the equivalent circuit in addition to the values of IE% that were calculated according to our previous work [25] are listed in Table 2.

According to usual convention, the parameters of the circuit shown in Fig. 7 can be defined as follows;  $R_s$  represents the solution resistance,  $R_p$  the polarization resistance, and  $Q$  the constant phase elements (CPEs). It can be seen from Fig. 6 that only one semicircle appear for all solutions and that the diameter of the diameter of the semicircle increases in the presence of the organic molecules and upon the increase of its concentrations. It is also seen from Table 2 that the reported values of  $R_s$  and  $R_p$  for iron in ATAT and TCDI containing solutions are higher than that obtain in chloride solution alone. The constant phase elements (CPEs,  $Q$ ) with their  $n$  values around 0.8 represent double layer

capacitors with some pores; the CPEs decrease upon addition and the increase of ATAT and TCDI concentrations. The CPE can be defined according to the following relation [59],

$$Z(\text{CPE}) = \left( \frac{Y_0 - 1}{(j\omega)^n} \right) \tag{14}$$

Here,  $Y_0$  is the CPE constant,  $\omega$  is the angular frequency (in  $\text{rad s}^{-1}$ ),  $j^2 = -1$  is the imaginary number and  $n$  is the CPE exponent.

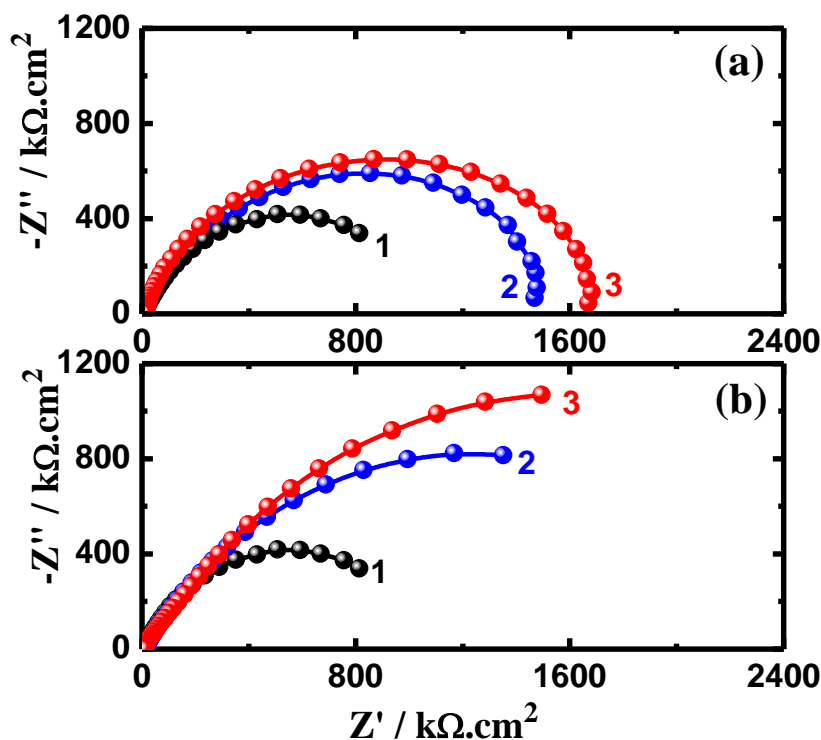


**Figure 6.** Typical Nyquist plots for iron electrode after its immersion for 60 min in 3.5% NaCl solutions without (1) and with (2)  $1 \times 10^{-3}$  M, and (3)  $2 \times 10^{-3}$  M (a) ATAT and (b) TCDI present, respectively.

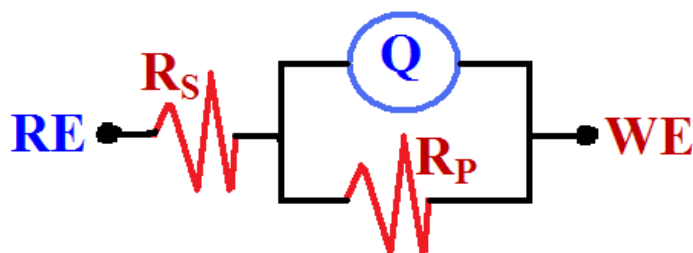


**Figure 7.** The equivalent circuit model used to fit the EIS experimental data.

Depending on the value of  $n$ , CPE can represent resistance ( $Z(\text{CPE}) = R$ ,  $n = 0$ ), capacitance ( $Z(\text{CPE}) = C$ ,  $n = 1$ ) or Warburg impedance for ( $n = 0.5$ ). The values of  $n$  in the present study were varying between 0.77 and 0.86 for all solutions, which means that the constant phase elements represent a capacitor but not pure due to the heterogeneity or the presence of little porosities in the formed layer on the iron surface.

The increase of  $R_s$ ,  $R_p$  and  $\text{IE}\%$  as well as the decrease of the CPE ( $Y_0$ ) values in the solutions containing increased concentrations of ATAT and TCDI indicate that these compounds are good corrosion inhibitors for iron in the 3.5% NaCl medium. This is attributed to the adsorption of ATAT and TCDI molecules on the iron surface protecting it from being corroded easily. The EIS results thus agree well with the data obtained by polarization, chronoamperometry, and open-circuit potential.

**Table 2.** EIS parameters obtained by fitting the Nyquist plots shown in Fig. 6 with the equivalent circuit shown in Fig. 7 for iron in 3.5% NaCl solutions in absence and presence of ATAT and TCDI, respectively.

Solution	Parameter				
	$R_s / \Omega \text{ cm}^2$	Q		$R_p / k \Omega \text{ cm}^2$	IE/%
		$YQ / \mu\text{F cm}^{-2}$	N		
NaCl alone	6.67	7.65	0.77	0.64	–
+ 1.0 mM ATAT	10.88	1.20	0.82	1.95	67.2
+ 2.0 mM ATAT	12.94	1.06	0.86	2.39	73.2
+ 1.0 mM TCDI	10.1	4.86	0.80	1960	67.3
+ 2.0 mM TCDI	12.7	4.11	0.80	3370	81.0

#### 4. CONCLUSIONS

The corrosion inhibition in 3.5% NaCl solutions of iron by the addition of  $1 \times 10^{-3}$  and  $2 \times 10^{-3}$  M of 3-amino-1,2,4-triazole-5-thiol (ATAT) and 1,1'-thiocarbonyldiimidazole (TCDI) was reported using the conventional dynamic polarization and chronoamperometric tests in a combination with electrochemical impedance spectroscopy and in situ Raman spectroscopy investigations. Results together showed that iron suffers both uniform and pitting corrosion in the chloride test solution. Iron first develop an adsorbed layer of ferrous hydroxide,  $\text{Fe}(\text{OH})_2$  converts to ferrite,  $\text{Fe}_3\text{O}_4$ . The ferrite is then attacked by chloride ions from the solution and transforms to ferric chloride,  $\text{FeCl}_3$ , which goes to the bulk solution causing the dissolution of iron. Addition of ATAT and TCDI to the chloride solution prevented the development of ferrous hydroxide and prevented the formation of ferrite due to the adsorption then polymerization of ATAT and TCDI molecules. This effect was greatly increased up on the increase of the organic compounds concentrations as a result of the increase of their adsorption onto the iron surface. This was confirmed by the decrease of the corrosion current and the corrosion rate and the increase of solution and polarization resistances for iron in the solutions containing increased concentrations of ATAT and TCDI. This was also proven by the in situ Raman spectra, which showed clearly the presence of ATAT and TCDI on the surface film formed on iron, while

immersed in the solutions containing their molecules. The percentage of the inhibition efficiency (IE%) was found also to increase by the increase of ATAT and TCDI concentration from  $1 \times 10^{-3}$  M to  $2 \times 10^{-3}$  M; the values of IE% obtained by polarization and impedance were almost close to each other at the same concentration. All measurements were in a good agreement stating clearly that ATAT and TCDI are good corrosion inhibitors against iron corrosion in 3.5% NaCl solutions and also the effect of ATAT as a corrosion inhibitor was nearly similar to that one obtained for TCDI.

#### ACKNOWLEDGEMENTS

The author extends his appreciation to the Deanship of Scientific Research at KSU for funding the work through the research group project No. RGP-VPP-160.

#### References

1. N.A. Al-Mobarak, *Int. J. Electrochem. Sci.*, 3 (2008) 666.
2. El-Sayed M. Sherif, R.M. Erasmus, J.D. Comins, *Electrochim. Acta*, 55 (2010) 3657.
3. J.L. Yao, B. Ren, Z.F. Huang, P.G. Cao, R.A. Gu, Z.-Q. Tian, *Electrochim. Acta*, 48 (2003) 1263.
4. A.N. Abdelhadi1, G.Y. Abbasi, F.M. Saeed, *Int. J. Electrochem. Sci.*, 5 (2010) 1665.
5. H. Amar, A. Tounsi, A. Makayssi, A. Derja, J. Benzakour, A. Outzourhit, *Corros. Sci.*, 49 (2007) 2936.
6. C.A. Melendres, N. Camillone III, T. Tipton, *Electrochim. Acta*, 34 (1989) 281.
7. El-Sayed M. Sherif, A.A. Almajid, *Int. J. Electrochem. Sci.*, 6 (2011) 2131.
8. M. Lebrini, F. Robert, C. Roos, *Int. J. Electrochem. Sci.*, 6 (2011) 847.
9. El-Sayed M. Sherif, *Int. J. Electrochem. Sci.*, 6 (2011) 5372.
10. El-Sayed M. Sherif, *J. Mater. Eng. Perform.*, 19 (2010) 873.
11. El-Sayed M. Sherif, *Int. J. Electrochem. Sci.*, 6 (2011) 2284.
12. El-Sayed M. Sherif, *Int. J. Electrochem. Sci.*, 7 (2012) 1482.
13. El-Sayed M. Sherif, *Int. J. Electrochem. Sci.*, 6 (2011) 3077.
14. S. Agnesia Kanimozhi, S. Rajendran, *Int. J. Electrochem. Sci.*, 4 (2009) 353.
15. El-Sayed M. Sherif, R.M. Erasmus, J.D. Comins, *J. Colloid Interface Sci.*, 306 (2007) 96.
16. V.F. Ekpo1, P.C. Okafor, U.J. Ekpe, E.E. Ebenso, *Int. J. Electrochem. Sci.*, 6 (2011) 1045.
17. El-Sayed M. Sherif, R.M. Erasmus, J.D. Comins, *J. Colloid Interface Sci.*, 309 (2007) 470.
18. E.E. Ebenso, I.B. Obot, L.C. Murulana, *Inter. J. Electrochem. Sci.*, 5 (2010) 1574.
19. El-Sayed M. Sherif, R.M. Erasmus, J.D. Comins, *Corros. Sci.*, 50 (2008) 3439.
20. E.F. Diaz, J.G. Gonzalez-Rodriguez, R. Sandoval-Jabalera, S. Serna, B. Campillo, M.A. Neri-Flores, C. GaonaTiburcio, A. Martinez-Villafañe, *Int. J. Electrochem. Sci.*, 5 (2010) 1821.
21. E.M. Sherif, S.-M. Park, *J. Electrochem. Soc.*, 152 (2005) B205.
22. El-Sayed M. Sherif, R.M. Erasmus, J.D. Comins, *J. Colloid Interface Sci.*, 311 (2007) 144.
23. E.M. Sherif, S.-M. Park, *J. Electrochem. Soc.*, 152 (2005) B428.
24. El-Sayed M. Sherif, *J. Appl. Surf. Sci.*, 252 (2006) 8615.
25. E.M. Sherif, S.-M. Park, *Corros. Sci.*, 48 (2006) 4065.
26. El-Sayed M. Sherif, A.H. Ahmed, Synthesis and Reactivity in Inorganic, *Metal-Organic and Nano Metal Chemistry*, 40 (2010) 365.
27. E.M. Sherif, S.-M. Park, *Electrochim. Acta*, 51 (2006) 4665.
28. E.M. Sherif, S.-M. Park, *Electrochim. Acta*, 51 (2006) 6556.
29. I. Lukovits, E. Kalman, F. Zucchi, *Corrosion*, 57 (2001) 3.
30. E.M. Sherif, S.-M. Park, *Electrochim. Acta*, 51 (2006) 1313.
31. El-Sayed M. Sherif, A.A. Almajid, F.H. Latif, H. Junaedi, *Int. J. Electrochem. Sci.*, 6 (2011) 1085

32. F.H. Latief, El-Sayed M. Sherif, A.A. Almajid, H. Junaedi, *J. Anal. Appl. Pyrolysis*, 92 (2011) 485.
33. El-Sayed M. Sherif, J.H. Potgieter, J.D. Comins, L. Cornish, P.A. Olubambi, C.N. Machio, *Corros. Sci.*, 51 (2009) 1364.
34. A.El Warraky, H.A. El Shayeb, E.M. Sherif, *Anti-Corros. Methods Mater.*, 51 (2004) 52.
35. Khalil A. Khalil, El-Sayed M. Sherif, A.A. Almajid, *Int. J. Electrochem. Sci.*, 6 (2011) 6184.
36. El-Sayed M. Sherif, A.A. Almajid, A.K. Bairamov, Eissa Al-Zahrani, *Int. J. Electrochem. Sci.*, 6 (2011) 5430.
37. El-Sayed M. Sherif, *Int. J. Electrochem. Sci.*, 6 (2011) 1479.
38. N. A. Darwish, F. Hilbert, W.J. Lorenz, H. Rosswag, *Electrochim. Acta*, 18 (1973) 421.
39. El-Sayed M. Sherif, A.M. El Shamy, M.M. Ramla and A.O.H. El-Nazhawy, *Mater. Chem. Phys.*, 102 (2007) 231.
40. J.H. Potgieter, P.A. Olubambi, L. Cornish, C.N. Machio, El-Sayed M. Sherif, *Corros. Sci.*, 50 (2008) 2572.
41. El-Sayed M. Sherif, J.H. Potgieter, J.D. Comins, L. Cornish, P.A. Olubambi, C.N. Machio, *J. Appl. Electrochem.*, 39 (2009) 1385.
42. El-Sayed M. Sherif, *J. Solid State Electrochem.*, 16 (2012) 891.
43. El-Sayed M. Sherif, *Int. J. Electrochem. Sci.*, 7 (2012) 1884.
44. El-Sayed M. Sherif, *Int. J. Electrochem. Sci.*, 7 (2012) 2374.
45. W. Li, K. Nobe, Arne J. Pearlstein, *Corros. Sci.*, 31 (1990) 615.
46. El-Sayed M. Sherif, *Mater. Chem. Phys.*, 129 (2011) 961.
47. M.M. Mennucci, E.P. Banczek, P.R.P. Rodrigues, I. Costa, *Cement Concrete Composites*, 31 (2009) 418.
48. P.G. Cao, J.L. Yao, J.W. Zheng, R.A. Gu, Z.Q. Tian, *Langmuir*, 18 (2002) 100.
49. F.V. Ruth, C. Paola, J.C. Rubim, S.M.L. Agostinho, *J. Electroanal. Chem.*, 472 (1999) 112.
50. N. Eldakar, K. Nobe, *Corrosion*, 33 (1997) 128.
51. J.R. Chin, K. Nobe, *J. Electrochem. Soc.*, 118 (1971) 545.
52. El-Sayed M. Sherif, A.A. Almajid, *J. Appl. Electrochem.*, 40 (2010) 1555.
53. El-Sayed M. Sherif, R.M. Erasmus, J.D. Comins, *J. Appl. Electrochem.*, 39 (2009) 83.
54. J.R. Macdonald, *Impedance Spectroscopy*, Wiley & Sons, New York, 1987.
55. El-Sayed M. Sherif, E.A. El-Danaf, M.S. Soliman, A.A. Almajid, *Int. J. Electrochem. Sci.*, 7 (2012) 2846.
56. El-Sayed M. Sherif, *Int. J. Electrochem. Sci.*, 7 (2012) 4235.
57. El-Sayed M. Sherif, *Int. J. Electrochem. Sci.*, 7 (2012) 2832.
58. El-Sayed M. Sherif, A.A. Almajid, A.K. Bairamov, Eissa Al-Zahrani, *Int. J. Electrochem. Sci.*, 7 (2012) 2796.
59. Z. Zhang, S. Chen, Y. Li, S. Li, L. Wang, *Corros. Sci.*, 51 (2009) 291.